Biochemical Journal (2019) **476** 3295–3312
https://doi.org/10.1042/BCJ20190576

PORTLAND PRESS

Research Article

Demonstration of a relationship between state transitions and photosynthetic efficiency in a higher plant

Craig R. Taylor*, Wim van Ieperen and Jeremy Harbinson

Department of Plant Sciences, Horticulture and Product Physiology, Wageningen University, 6708 PB Wageningen, The Netherlands

Correspondence: Craig R. Taylor (taylor.craigr@ymail.com)

A consequence of the series configuration of PSI and PSII is that imbalanced excitation of the photosystems leads to a reduction in linear electron transport and a drop in photosynthetic efficiency. Achieving balanced excitation is complicated by the distinct nature of the photosystems, which differ in composition, absorption spectra, and intrinsic efficiency, and by a spectrally variable natural environment. The existence of long- and short-term mechanisms that tune the photosynthetic apparatus and redistribute excitation energy between the photosystems highlights the importance of maintaining balanced excitation. In the short term, state transitions help restore balance through adjustments which, though not fully characterised, are observable using fluorescence techniques. Upon initiation of a state transition in algae and cyanobacteria, increases in photosynthetic efficiency are observable. However, while higher plants show fluorescence signatures associated with state transitions, no correlation between a state transition and photosynthetic efficiency has been demonstrated. In the present study, state 1 and state 2 were alternately induced in tomato leaves by illuminating leaves produced under artificial sun and shade spectra with a sequence of irradiances extreme in terms of PSI or PSII overexcitation. Light-use efficiency increased in both leaf types during transition from one state to the other with remarkably similar kinetics to that of F′m/Fm, F′o/Fo, and, during the PSII-overexciting irradiance, Φ_{PSII} and q_P. We have provided compelling evidence for the first time of a correlation between photosynthetic efficiency and state transitions in a higher plant. The importance of this relationship in natural ecophysiological contexts remains to be elucidated.

Introduction

The optimal light-use efficiency of photosynthesis depends on the optimal excitation of photosystems I and II. This arises from the need to balance linear (through PSII and PSI) and cyclic (around PSI) electron transport fluxes (yielding reduced ferredoxin and then NADPH) and their associated proton transport fluxes (yielding ATP synthesis) with the demands of metabolism and the activity of the Mehler reaction. In the case of C3 plants linear electron transport predominates under most circumstances. The stoichiometry of proton release into the thylakoid lumen that occurs together with linear electron transport, together with the 14/3 proton:ATP ratio expected for the chloroplast ATPase, results in an ATP/NADPH ratio of ~1.28. This is close to the ATP/NADPH demand of 1.5 for CO_2 fixation alone, and the demand of 1.75 for photorespiration alone [1]. The shortfall in ATP is made up by alternative electron transport activity (cyclic electron transport and the Mehler reaction) and the low ATP/Fd demand of other reductive metabolic activities such as nitrite reduction, sulfate reduction, fatty acid biosynthesis, and the export of reducing power from the chloroplast. Maximally efficient linear electron transport depends on the balanced electron transport through the two photosystems; this will require, however, overexcitation of PSII relative to PSI as the quantum yield for

*Current address: Unit 3 Village Artisan, 69 Cabriere Street, Franschhoek, 7680, Western Cape, South Africa

Received: 14 August 2019
Revised: 9 October 2019
Accepted: 9 October 2019

Accepted Manuscript online: 10 October 2019
Version of Record published: 11 November 2019

Biochemical Journal (2019) 476 3295–3312
https://doi.org/10.1042/BCJ20190576

electron transport by PSI is higher (~0.99) than PSII (~0.88; based on fluorescence data and accounting for the PSI fluorescence error in the determination of Fo and Fm [2]). In the event that some of the ATP shortfall were to be made up from cyclic electron transport rather than pseudocyclic electron transport or the extra ATP arising from the activity of photosynthetic reduction processes (like nitrate reduction) with a low ATP/Fd demand, then overall excitation of PSI would need to be increased relative to that of PSII.

A further problem affecting the optimal operation of photosynthesis is that the two photosystems do not have an identical light absorption spectrum and spectral light-use efficiency [3]. These differences arise from differences in the pigments and the binding of pigments in the two photosystems to which should be added the lower energy transfer to chlorophyll of carotenoids compared with that of chlorophyll to chlorophyll [4]. Overall, it seems that at most photosynthetically active wavelengths there is an overexcitation of PSII relative to PSI. The spectrum of light incident on a leaf is not constant but highly variable due to, amongst other things, sun angle, weather, and intermittent shading by other leaves [5]. It follows, therefore, that spectrum and changes in the spectrum has great potential to disrupt the balanced activities of PSI and PSII required for optimal linear electron transport.

Optimum light-use efficiency — the optimal excitation of the two photosystems — is critical in any situation where light is limiting, such as low irradiances. Maintaining this optimal excitation is, however, difficult because of the changing metabolic demands changing the need for cyclic electron transport, and changing the spectrum of the irradiance combined with the absorption and photophysical properties of the two photosystems. Plants possess mechanisms to balance, at least to some extent, photosystem excitation. These range from longer-term adjustments of photosystem ratio and composition to short-term adjustments in pigment-binding protein associations between the two photosystems. In the order of days, leaves acclimate to the growth spectrum by tuning the relative amounts of the photosystems and associated light-harvesting complexes [6,7]. The long-term nature of this kind of adjustment is demonstrated by the 'memory' of leaves produced under a spectrum that preferentially excites PSI or PSII: leaves show a comparatively higher photosynthetic efficiency when exposed to an irradiance which, in terms of spectral composition and absorption by the photosystems, more closely matches that of the growth spectrum [6].

State transitions represent a considerably faster excitation-balancing mechanism, operating over minutes in response to imbalances in electron transport through PSI and PSII. This reversible process is defined by two states — 'state 1' and 'state 2' — which reference one of two putative docking positions of a potentially mobile LHCII pool [8]. The classical view of state transitions is that, in state 1, mobile LHCII becomes associated with PSII during periods of PSI overexcitation whereas in state 2 LHCII becomes associated with PSI during periods of PSII overexcitation with the redox state of the PQ pool being pivotal in the regulation of the state transition process [9]. In accordance with this model, a state transition regulates the cross-sectional area of PSI and PSII in a reciprocal manner and helps restore balance by enhancing light capture by the rate-limiting photosystem whilst limiting light capture by the overexcited photosystem. Of the three LHCII apoproteins (viz. Lhcb1, Lhcb2, and Lhcb3), Lhcb1 and Lhcb2 can be phosphorylated in a process which requires the STN7 kinase in plants, and the Stt7 kinase in algae, which itself is believed to be activated by a reduced PQ pool [10]. It is this phosphorylation of LHCII that induces mobility of a proportion of LHCII and results in state 2. A return to state 1 occurs when an oxidised PQ pool triggers dephosphorylation of Lhcb1 and Lhcb2 in a process that is less well understood, although the phosphatases TAP38 and PPH1 have been shown to play a role in this regard [11,12]. A potential overcapacity of electron transport through PSII will result in the reduction in Q_A, which will result in an increasing reduction in the PQ pool, potentially until the quantum yield of PSII decreases to bring actual electron transport activity into balance with that of PSI. A potential overcapacity of electron transport through PSI will result in oxidation of the intersystem electron transport chain, including the PQ pool, until the oxidation of P700 increases to the point where the quantum yield of PSI falls to match the flux of electrons from PSII and cyclic electron transport.

The biochemical reorganisation which occurs during a state transition is readily detectable in algae, cyanobacteria and higher plants using spectroscopic [13–15], photoacoustic (e.g. [16–19]) and proteomic methods [9]. Chlorophyll fluorescence, for example, reveals distinct kinetics upon transition from state to the other [20]. When state 1 leaves (i.e. fully adjusted to an overexcitation of PSI) are presented with so-called PSII light (light which over-excites PSII and induces a transition to state 2) fluorescence yield increases sharply and is gradually quenched until a new equilibrium in state 2 is achieved. Subsequently presenting state 2 acclimated leaves with PSI light (light which over-excites PSI) is met with a sharp decrease in fluorescence yield followed by a gradual increase in fluorescence yield to a new steady state as a return to state 1 occurs. The changes in PSII antennae

Biochemical Journal (2019) 476 3295–3312
https://doi.org/10.1042/BCJ20190576

size during state transitions can be estimated by changes in Fm and Fo between the two states [20]. In the algae *Chlorella pyrenoidosa*, light absorption by PSII is reduced by an estimated 10% when in state 2 compared with state 1 [13] and a similar reduction in 10–15% has been reported in the cyanobacteria *Nostoc muscorum* which was accompanied by an equivalent increase in PSI antennae size [19]. Following a transition to state 2 in higher plants, decreases in PSII antennae size of 11% [21] and 20% [22] have been reported and an increase in PSI antennae size of 12% has been determined by 820 nm absorbance changes [23].

The precise location of LHCII and its three trimers in state 1 and state 2 is, however, the subject of contrasting findings that do not match with the classical model. In isolated spinach chloroplasts, for example, mobile LHCII was attached to PSII in state 1 but was not associated with PSI in state 2 [24]. Picosecond-fluorescence spectroscopy of the algae *Chlamydomonas reinhardtii* showed that only a negligible amount of mobile LHCII docks with PSI [25]. It has recently become possible to better purify PSI-LHCII complexes and, using this approach, mobile LHCII has been shown to be an intimate part of PSI rather than that of PSII as widely believed [26]. Moreover, those authors showed that mobile LHCII is a very effective antenna for PSI in state 2. An alternative finding is that mobile LHCII serves as an antenna of both photosystems and this allows for acclimation to different growth light intensities simply by regulating the amount of LHCII [27].

Whatever the precise points of attachment are for mobile LHCII in either of the states, the perceived role of state transitions as an acclimatory mechanism whose purpose is to alleviate, or at least partially alleviate, photosystem excitation imbalance has gained widespread acceptance based on current evidence [9]. It is reasonable to predict that as state transitions act to optimise the balance of excitation of PSII and PSI, they ought also to positively influence the rate of CO_2 assimilation and hence photosynthetic efficiency. In seminal work describing the phenomenon of a state transition, Bonaventura and Myers [13] observed a relationship between state transitions and oxygen evolution in *C. pyrenoidosa*. Those authors observed an accompanying increase in oxygen evolution with similar kinetics to that of fluorescence yield which reveals a clear functional role for state transitions that is congruent with its effects at the level of electron transport. Arabidopsis lacking the STN7 kinase and consequently unable to perform state transitions showed decreased biomass under changeable light conditions, demonstrating the significance of state transitions at the whole-plant level [10]. In another alternating PSI/PSII light regime the stn7 mutant produced half as much seed as the wild-type, further indicating a benefit to plant fitness [28]. The same mutants produced 19% less seed than their wild-type counterpart in field conditions, showing the significance of state transitions under natural conditions [29]. However, a study of the responses of assimilation to irradiance expected to induce changes between states 1 and 2 showed no alterations in the assimilation of the kind expected to accompany a state transition, despite bearing the same fluorescence signatures associated with state transitions in algae [15]. It has, therefore, been suggested that the apparent beneficial effects of state transitions at the whole-plant level cannot be quantified using gas exchange measurements [30]. The apparent disconnection between responses at the thylakoid level and those of assimilation in relation to state transitions has posed problems for understanding the significance and impact of state transitions. We re-examine the possible relationship between state transitions and photosynthetic efficiency by inducing an extreme photosystem excitation imbalance. We show that, under these extremes, changes at the molecular level that occur during a state transition are correlated with changes in the rate of CO_2 fixation and quantum yield. This not only partly resolves the puzzle of the lack of an effect of state transitions at the level of assimilation but also offers a new, relatively straightforward way of monitoring state transitions in terms of extent and kinetics.

Materials and methods

Plant material and growth environment

Tomato seeds (*cv.* Moneymaker) were sown in rockwool blocks (Grodan, Roermond, The Netherlands) and divided equally into two light-tight plastic-lined fabric enclosures (80 cm × 80 cm × 50 cm) in a climate-controlled room (16-h photoperiod, 20°C air temperature, 70% relative humidity). Rockwool blocks were irrigated from below with Hoagland solution via pumps which operated for 15 min once per day. Each enclosure was illuminated with a different light source to provide spectrally distinct growth environments. The light sources used were a plasma lamp (Plasma International, Muhlheim am Main, Germany) and a quartz-halogen lamp assembly comprising four floodlight housings, each fitted with 500 W lamps (Osram, Munich, Germany). The plasma lamp provided a daylight-like spectrum (hereafter referred to as 'SUN') whereas light from the quartz-halogen lamps was diffused with a ground glass diffuser and filtered with a plastic-film filter (type 'cold

Biochemical Journal (2019) 476 3295–3312
https://doi.org/10.1042/BCJ20190576

blue', Lee Filters, Andover, U.K.) to provide a shade-like spectrum (hereafter referred to as 'SHADE', see [7]). Figure 1 shows the relative quantum flux and spectral distribution of each of these light sources together with that of the two narrowband actinic irradiances used for gas exchange measurement (see 'Actinic light' section below). The lighting environments were selected based on their expected influence on photosystem excitation balance; the SUN spectrum over-excites PSII whereas the SHADE spectrum over-excites PSI. The enclosures were impervious to light to ensure no spectral contamination from adjacent enclosures. The intensity of light incident on the apical buds of the seedlings, and subsequently the third leaf once it began to develop, was controlled at 100 μmol m^{-2} s^{-1} ±5% by measuring the irradiance using a Licor quantum sensor (Li-190, LI-COR, NE, U.S.A.) and adjusting plant height. It was observed that leaves tended to droop and no longer be normal to the direction of the incident irradiance. To ensure that the third leaf received the desired irradiance it was supported normal to the light using wooden stakes from below. Poor germination rates were observed in the shadelight treatment. To remedy this, seeds destined for the shadelight treatment were allowed to germinate in the daylight treatment and transferred to the shadelight treatment once the cotyledons had fully expanded.

Fans within the enclosures provided air circulation around the plants and fans mounted in the walls of growth enclosures ventilated the enclosures. The high heat output from the quartz-halogen lamp compared with the plasma lamp had the potential to create large differences in leaf temperature between the treatments. The amount of ventilation for each enclosure was adjusted to ensure that leaf temperature was 22.5 ± 1°C in the growth enclosures.

Gas exchange

A custom two-part gas exchange chamber, similar to that described in [31], was used for gas exchange measurements. The main difference compared with the previous design is a slightly reduced chamber area (3.80 cm^2). The gas mix used for measurement comprised 400 μmol mol^{-1} CO_2, 20 mmol mol^{-1} O_2 (i.e. 2% O_2), and 18.8 mmol H_2O with the remainder being N_2. The gas stream was split into reference and sample streams with the sample stream being sent to the leaf chamber and then to the gas analysis system. The reference stream was analysed by a Li-7000 CO_2/H_2O analyser (LI-COR, NE, U.S.A.) operating in absolute mode while the difference between the mole fractions of the absolute and relative gas streams was measured by a Li-7000 CO_2/H2O analyser operating in differential mode. The differential accuracy of the Li-7000 analysers was compared against a Li-6400 (LI-COR, NE, U.S.A.) by flowing the incoming and exhaust gas over the analysers in the Li-6400 head. The test showed that the differential reading for both analysers and Li-6400 was in agreement to >0.1%. A flow rate of 250 ml min^{-1} was used for all measurements and was sufficient for CO_2 depletion rates to remain within ∼10 μmol mol^{-1}. The accuracy of the flow was verified by cross-checking it with a newly calibrated flow meter (Bronkhorst, Ruurlo, The Netherlands). Flow rates were within 0.2% for the two flow meters used. The same flow meter used for cross-checking the chamber flow was then placed in series with the exhaust gas to test for the presence of leaks with and without a leaf in the chamber. Tests showed that gas leaks originated from the lower seal due to imperfect seals around leaf veins. A liquid, two part, non-toxic, skin-safe, quick-setting (∼5 min working time) moulding silicone rubber applied between the lower foam rubber chamber seal and the lower leaf surface (Body Double Fast Set, Allentown, PA, U.S.A.) immediately before closing the chamber eliminated all detectable leaks. Each day, before commencing measurements, standard gases comprising 491 ppm CO_2 (±2 ppm) and N_2 or pure N_2 were flowed separately through the analysers to test for calibration drift. Oxygen concentration was then verified using an oxygen analyser (type 570A, Servomex, Crowborough, U.K.). Leaf temperature was monitored using a non-contact temperature sensor (Micro IRt/c, Exergen, Watertown, MA, U.S.A.) directly below the leaf. In a separate test, the accuracy of the temperature sensor was verified using a type K thermocouple appressed to the abaxial surface of the leaf. This type K thermocouple had been shown to measure within 0.1°C of an Omega high accuracy thermistor probe (Omega, Norwalk, CT, U.S.A.). Leaf temperature was maintained at 22.5°C by circulating water from a temperature-controlled water bath through an internal channel in the upper and lower chamber halves.

Actinic light

Actinic light was chosen to induce state 1 (PSI light, LHCII (largely) connected to PSII) or state 2 (PSII light, some LHCII potentially connected to PSI). Irradiance with a nominal peak wavelength of 480 or 700 nm (Figure 1) was used as PSII and PSI light, respectively. These irradiances were chosen based on prior measurements which showed that, of 15 narrowband wavelengths spread across the PAR spectrum, 480 nm irradiance most strongly excites PSII whereas 700 nm irradiance most strongly excites PSI (while driving photosynthesis

Biochemical Journal (2019) 476 3295–3312
https://doi.org/10.1042/BCJ20190576

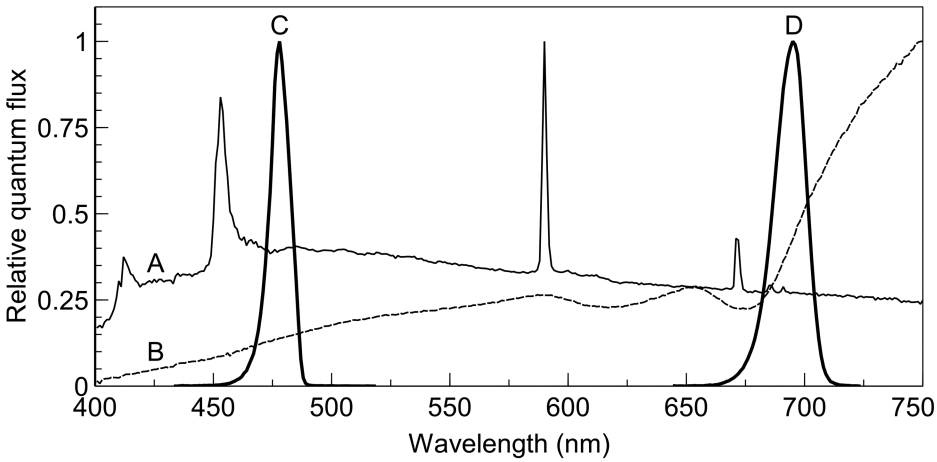

Figure 1. Spectra of growth and measurement light.

Relative quantum flux and spectral distribution of (A; thin solid line) artificial daylight spectrum, (B; dotted line) artificial shade spectrum, (C; left thick line) filtered 480 nm (nominal) irradiance (peak wavelength 478, 10 nm FWHP), and (D; right thick line) 700 nm (nominal) irradiance (peak wavelength 695, 10 nm FWHM). The broadband spectra were used as growth irradiance treatments and the narrowband spectra were applied separately as actinic irradiance during gas exchange measurements.

sufficiently strongly to avoid the problem of a low signal to noise ratio from the gas analysers). PSII light was produced using an array of 470 nm LEDs (LXZ1-PB01, Lumileds, San Jose, CA, U.S.A.) on a metal-cored PCB in combination with a 480 nm interference filter (10 nm FWHM, Thorlabs, Newton, NJ, U.S.A.) and PSI light was produced using a 700 nm LED (LED700-66-60, Roithner Lasertechnik, Vienna, Austria) in combination with a 700 nm interference filter (10 nm FWHM, Thorlabs, Newton, NJ, U.S.A.). Each LED was mounted on a heatsink with forced air cooling to avoid the intensity shifts associated with increases in LED junction temperature upon switching. LED-heatsink assemblies and filters were secured on a laboratory-built optical bench which comprised a blower to force air across the filters to minimise increases in filter temperature upon switching and maintain the stability of their optical characteristics. The two actinic light LEDs were coupled to the chamber using a branched fibre-optic bundle with an output diameter of 25 mm. A 15 cm long transparent acrylic 25 mm diameter rod was placed at the output of the fibre to ensure that light distribution at leaf level was homogenous.

Two irradiance sensors were built and used to measure irradiance in the leaf chamber; one was used for routine measurement of irradiance incident on the leaf (sensor 1) and the other (sensor 2) was used for calibration purposes. Sensor 1 was made from a light guide with a diameter of 3 mm, which extended into the leaf chamber above the leaf and into the path of actinic light. This light guide was coupled to an external photodiode (OSD15-5T, Centronic, Croydon, U.K.) whose photocurrent was translated to a voltage by a transimpedance amplifier. Sensor 1 was calibrated *in situ* using sensor 2, a laboratory-built sensor comprising 13 three millimetre diameter photodiodes (TEFD4300, Vishay, Coatesville, PA, U.S.A.) embedded concentrically and evenly across a sensing area identical with that of the cross-sectional measurement area of the chamber. This laboratory-made sensor was calibrated against a calibrated CL500a illuminance spectrophotometer (Konica Minolta, Tokyo, Japan) and a LiCor quantum sensor (Li-188, NE, U.S.A.). The calibration wavelengths used consisted of a 'white' broadband spectrum and 22 narrowband wavelengths in the range 380–740 nm which included the two narrowband spectra (480 and 700 nm) used in this study. The calibration procedure was repeated twice to test for consistency; the readings of sensor 2 for each calibration run were found to be identical. The readings of the Licor quantum sensor were on average 3% higher than those of the spectrophotometer for the narrowband spectral distributions lying within the sensitivity region of the quantum sensor (i.e. PAR region) with an 11% overestimation at 422 nm and a 6% underestimation at 519 nm. The CL500a was used as the calibration reference for the laboratory-made sensor 2 since it is known that the LiCor quantum sensor does not have a flat sensitivity across the PAR spectrum and because the CL500a is spectrally resolved and designed to measure accurately for narrow bands across its range of sensitivity. The CL500a also allowed for calibration of sensor 2 outside of the PAR region which is of importance to this study.

Biochemical Journal (2019) 476 3295–3312
https://doi.org/10.1042/BCJ20190576

Since the polyacrylamide plastic body of sensor 2 had a significantly higher reflectance than the tomato leaves to be measured, it caused more light to be reflected onto chamber walls and back onto itself; the sensor and the upper part of the leaf chamber formed a cavity resulting in overestimation of irradiance relative to the same system with a leaf in place of the white diffuser of the sensor. This was corrected for each irradiance by comparing the irradiance intensity transmitted by glass fibre surrounded by a punched leaf with that obtained using a polyacrylamide disk in place of the leaf. The 4 mm diameter window of the glass fibre was positioned in the centre of the chamber (at leaf level) and transmitted light to a USB2000 spectrophotometer (Ocean Optics, Duiven, The Netherlands). The percentage differences in irradiance intensity using either the leaf or polyacrylamide disk did not exceed 4% for any of the irradiances and sensor 2 was corrected accordingly for the wavelength-dependent reflection component associated with these irradiance intensity measurements. Sensor 1 was, in turn, calibrated against the corrected sensor 2 and used for routine measurements of irradiance with a leaf *in situ*. Another optical difference between the leaf and sensor 2 was that some light could transmit through the leaf to the lower chamber and, by reflection onto the abaxial side and re-transmission through the leaf, could interact with sensor 1. However, these second-order reflections from the lower chamber were negligible and ignored.

Chlorophyll fluorescence

Chlorophyll fluorescence was determined using a laboratory-built modulated system. Fluorescence was excited by the application of a red measuring beam with an intensity of 0.25 μmol m^{-2} s^{-1}, produced using a red LED (660 nm peak emission) which was filtered (660 nm) and modulated at ∼1 kHz (the exact frequency was adjusted to minimise interference from background electrical noise). The excitation beam was coupled to the leaf chamber using a fibre-optic light guide and a hot mirror was attached to the leaf-chamber end of the fibres to remove fibre fluorescence which otherwise results in a slightly lowered dark-adapted Fv/Fm. When required, a saturating light pulse with an intensity of ∼12 000 μmol m^{-2} s^{-1} was generated using three high power red LEDs (Phlatlite, Sunnyvale, CA, U.S.A.) controlled by a laboratory-built timer based on a PIC microcontroller (Microchip Technology, Chandler, AZ, U.S.A.). Three fibre-optic light guides, one per LED, delivered the saturating light pulse through three side ports of the leaf chamber. Chlorophyll fluorescence was detected by three GaAsP photodiodes (G1736, Hamamatsu, Hamamatsu City, Japan) spaced evenly below the leaf. Each photodiode was filtered with an RG-9 filter (3 mm, Schott, Mainz, Germany) to screen them from filtered excitation light and other short-wavelength irradiances. The photocurrent from these fluorescence sensing photodiodes was pre-amplified using transimpedance amplifiers based on OPA627 operational amplifiers (Texas Instruments, Dallas, TX, U.S.A.). Laboratory-built phase-sensitive detectors further amplified and recovered the fluorescence signals, which were then recorded using a data logger (National Instruments, Austin, TX, U.S.A.) with a 10 Hz low-pass filter on its inputs to further smooth the signals. The maximum quantum efficiency of PSII (Fv/Fm) was determined at the start and end of measurements. Minimum fluorescence (Fo) (i.e. that measured in the dark-adapted state) was determined after the leaf had been subjected to at least 20 min of darkness in the leaf chamber and immediately before the measurement of Fm. Light-adapted minimum fluorescence (F′o) was determined by interrupting actinic light and providing a 1 s far-red pulse to oxidise all Q_A and so get an accurate F′o. Calculations of Φ_{PSII}, F′v/F′m, and NPQ were made according to [32].

Measurement procedure

Measurements were taken on third, fully expanded leaves, at ∼30–35 days after sowing. Leaves were placed in the leaf chamber and allowed to dark-adapt for 20 min to determine the rate of dark respiration and Fv/Fm. All leaves used for measurement were healthy with a Fv/Fm > 0.8. Actinic light was then applied, commencing with PSII light, and then alternating with PSI light at 65-min intervals. Light intensities were carefully chosen to meet three criteria: to be sufficiently high to avoid any non-linearity occurring at very low intensities [33], to be well within the strictly light limiting region, and to ensure that CO_2 assimilation rates were comparable for PSI and PSII light to avoid any confusion of state transitions (or other changes) with any intensity-dependent effects (such as photosynthetic induction) upon changing from one light source to the other.

To be sure that the PSI and PSII light produced similar assimilation rates, tests were performed on SUN and SHADE leaves in which PSI light was adjusted so that the steady state assimilation rate matched that developed under a reference absorbed PSII light intensity of 40 μmol m^{-2} s^{-1}. The required PSI-light intensities were 55.6 μmol m^{-2} s^{-1} for SUN leaves and 53.9 μmol m^{-2} s^{-1} for SHADE leaves. The measurements were divided into two sets. In one set of measurements, the rate of CO_2 depletion for three replicate leaves was determined

Biochemical Journal (2019) 476 3295–3312
https://doi.org/10.1042/BCJ20190576

with fluorescence measuring beams switched on but actinic light was not interrupted at any point throughout the measurement and saturating pulses were not applied. This had the obvious drawback that only Fs could be determined but ensured that CO_2 depletion traces were smooth and unaffected by disruptions to stable measurement conditions. A second set of measurements included simultaneous measurements of all basic chlorophyll fluorescence parameters at 0.5, 3, 6, 9, 12, 15, 20, 25, 30, 40, 50, and 60 min after switching from one light to the other, except for the PSII light application following dark adaptation where fluorescence measurements were taken at 50 and 60 min. In this latter group of measurements, the responses of the assimilation to PSI or PSII light is less clear because of the superimposed saturating irradiances and interruptions in irradiance.

Leaf light absorption

Leaf light absorption for each leaf was taken as the average absorption of three disks which were punched from the area of the leaf that had been in the gas exchange chamber. The leaf absorption apparatus comprised two integrating spheres (50 mm diameter reflectance and transmittance spheres; Avantes, Appeldoorn, The Netherlands), one used for measurement of leaf light transmission and the other for leaf light reflection. These spheres were used in a light-tight enclosure. The leaf disks were clamped into an aluminium holder that fitted securely to each integrating sphere, positioning the disks above the measurement ports. Leaf transmittance and reflectance were measured using a broadband light source comprising two LED sources; one a warm white LED and the other a blue light source consisting of four LEDs that generated peak wavelengths of 380, 400, 420, and 440 nm (Mightex Systems, Toronto, Canada) to provide improved signal to noise ratio in the blue region. These light sources were coupled to a branched glass fibre which was connected to the measuring light inlet port (angled at 8° to the vertical) of the reflectance sphere, or held at 8° to the vertical and the light focused and directed to the middle of the measurement port of the transmittance sphere. Transmission and reflectance measurements, including the transfer of each disk and light source from one sphere to the other, usually took no longer than 2 min. In such a short time period, any chloroplast movement induced by the high intensity broadband measurement light does not interfere to any significant extent on transmission and reflectance measurements. Two spectrometers (USB-4000, Ocean Optics, Dunedin, FL, U.S.A.), one per sphere, analysed the transmitted and reflected light with a spectral resolution of 0.2 nm. Leaf absorption was obtained by subtracting transmittance and reflectance values from 1.0. This provided a static, post-measurement leaf light absorption value. To determine how leaf absorption might have changed during gas exchange measurement, SUN and SHADE leaves were placed over the port of an integrating sphere (LiCor 1800-12, LiCor, Lincoln, NE, U.S.A.) and subjected to the same irradiance regime that was used for gas exchange. Transmission measurements were taken separately and logged at each of the time intervals used for gas exchange, using the same configuration described for post-measurement absorption measurement. Reflectance was estimated using the relationship between transmission and reflectance data from the post-measurement leaf light absorption measurements.

Results

Basic characterisation of SUN grown and SHADE grown plants

SHADE grown plants were considerably more etiolated than SUN grown plants (Supplementary Figure S1). The chlorophyll *a*/*b* ratio, determined by fitting an 80% acetone extract absorption spectrum to that of known absorption spectra for individual pigments [34], was higher in SUN plants (3.08) than in SHADE plants (2.89) (Supplementary Figure S2).

Gas exchange

Rates of assimilation for SUN and SHADE leaves are shown in Figure 2. When leaves were exposed to PSII light following dark adaptation, assimilation increased until a steady state was reached. Upon switching from PSII light to PSI light, a sharp drop in gas exchange occurred, reaching a local minimum at ~3 min after the change. The assimilation rate then recovered, increasing over ~50 min to a steady state similar to that achieved under PSII light. After switching from PSI to PSII light, the assimilation rate once again decreased and subsequently recovered. However, the drop following a change from PSI light to PSII light is considerably deeper than occurs during the PSII light to PSI light alternations and, furthermore, the recovery is faster with steady state being reached after ~30 min. The spikes in assimilation which occurred upon switching from PSII to PSI

Biochemical Journal (2019) 476 3295–3312
https://doi.org/10.1042/BCJ20190576

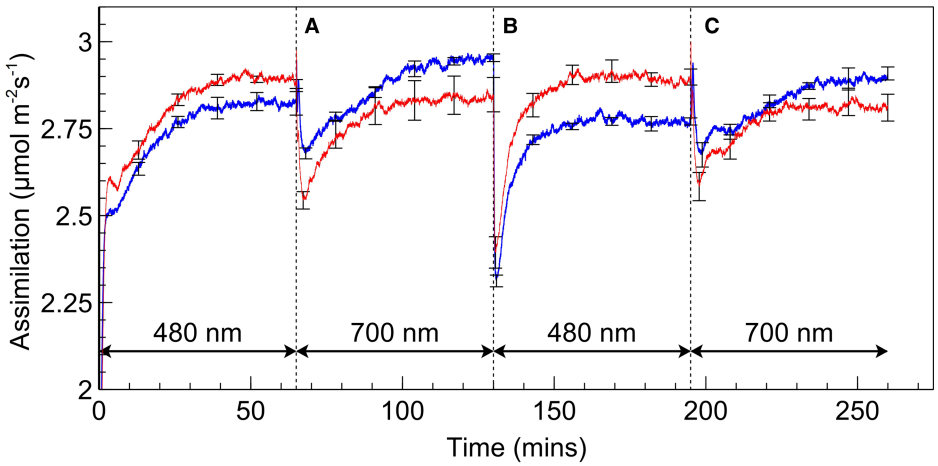

Figure 2. Assimilation rates during a PSII/PSI light regime.

Rates of assimilation for SUN (red) and SHADE (blue) leaves during a PSII/PSI light regime. Absorbed irradiance was 40 µmol m^{-2} s^{-1} for each irradiance type. Letters 'A', 'B', and 'C' are references for Figure 3. Error bars shown represent the SEM ($n = 3$).

light are conspicuous; more detailed analysis of these spikes (Figure 3) reveals a bimodal response of assimilation when switching from PSII light to PSI light; the falling edge of the initial spike is met with a more rounded peak which is generally of lesser magnitude than the spike preceding it. These kinetics occurred within ~1 min after switching and assimilation subsequently dropped to a local minimum (~2–3 min after switching) prior to commencement of recovery in assimilation rate. No such kinetics were observed when switching from PSI to PSII light; assimilation dropped sharply to a local minimum within 1 min.

We chose irradiances for PSI and PSII light that resulted in nearly identical steady state assimilation rates in order to minimise photosynthetic induction as a potential contributing factor to the observed recoveries in assimilation after switching of irradiance. Nonetheless, a switch from PSII light to PSI (or back) could potentially produce local photosynthetic induction kinetics because of the different absorption profiles of the two irradiances within the leaf. When alternating to PSI light from PSII light, for example, the PSI light, which is more weakly absorbed by the leaf, more strongly illuminates deeper cell layers. The latter could produce a

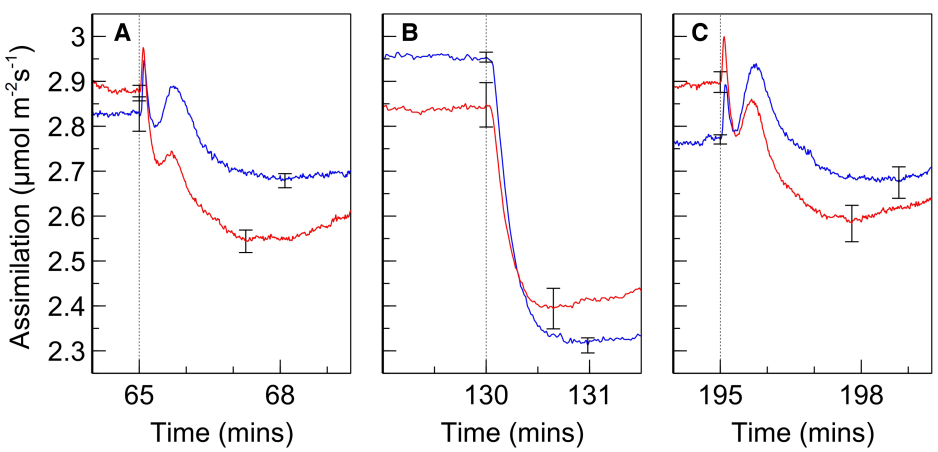

Figure 3. Detailed view of assimilation rates upon light switching.

(**A–C**): Detailed view of assimilation rate in SUN (red) and SHADE (blue) leaves during (**A**) switching from PSII to PSI light, (**B**) switching from PSI to PSII light, and (**C**) second switching from PSII to PSI light. Letters correspond with data segments by 'A' and 'B' in Figure 2. Error bars shown represent the SEM ($n = 3$). The set of error bars to the right of the dotted line correspond with local minima after switching.

Biochemical Journal (2019) **476** 3295–3312
https://doi.org/10.1042/BCJ20190576

photosynthetic induction response in those cells, creating a slow increase in the rate of assimilation that is not associated with a state transition. On the other hand, the alternation from PSI light to PSII light, which is more strongly absorbed by the leaf, would result in upper cell layers absorbing considerably more quanta which could also induce a photosynthetic induction.

To more fully exclude photosynthetic induction as a contributing factor to the observed increases in assimilation after a wavelength change, a leaf was exposed to a sequence of PSII and PSI light at half the intensity, followed by the same intensity, used to obtain the results in Figure 2 (Figure 4). The same characteristic induction in assimilation was observed when the leaf was first exposed to PSII or PSI light but upon doubling the irradiance the rate of assimilation increases to a new, stable, rate without any of the kinetics observed following a change in wavelength. The short-lived spikes in assimilation upon the doubling of irradiance intensity were further investigated by examining light intensity upon switching but were found to be physiological in nature and not due to an overshoot in irradiance.

Although irradiance intensities were intentionally low and consequently thought unlikely to induce chloroplast movement and associated changes to leaf light absorption, it was nonetheless important to exclude this as a contributing factor to the observed recovery in assimilation after a change in the illumination spectrum. Results for light transmission, reflectance, and absorbance obtained *in situ* (i.e. when in the leaf chamber) from intact leaves subjected to PSII, and subsequently PSI, light are shown in Figure 5. Transmission and reflectance in dark-adapted SUN and SHADE leaves increased when exposed to PSII light and subsequently decreased when exposed to PSI light. Calculated leaf light absorption for SUN leaves decreased by 2.2% during exposure to PSII light and increased by 2.1% during subsequent exposure to PSI irradiance. The corresponding changes in leaf light absorption for SHADE leaves were 3.8% and 3.1%. In the absence of any other changes, it is expected that the effect of these changes in leaf absorption would be to decrease assimilation during PSII light exposure as well as to increase assimilation during subsequent exposure to PSI. Φ_{CO2} is a measure of the integrated light-use efficiency of photosynthesis. Figure 6 shows Φ_{CO2} using either (A) a single light (broadband 'white' light) absorption of leaf discs measured immediately after the gas exchange measurement i.e. a 'static' absorption value or (B) the light absorption of the leaves calculated throughout the measurement of assimilation based on actual leaf light transmission changes i.e. 'dynamic' absorption values. After correcting Φ_{CO2} for the changes in leaf light absorption there remains a recovery in Φ_{CO2} after exposure of PSII light or PSI light. Owing to the difference in leaf absorption values obtained using either the static or dynamic approaches the quantitative effect of the correction differs between these treatments, but not the existence of the recovery of Φ_{CO2} itself.

Fluorescence measurements

The fluorescence yield when leaves were transferred from one irradiance to the other (Figure 7) showed distinct kinetics associated with state transitions [9,13]. The application of PSII light following PSI light exposure, when

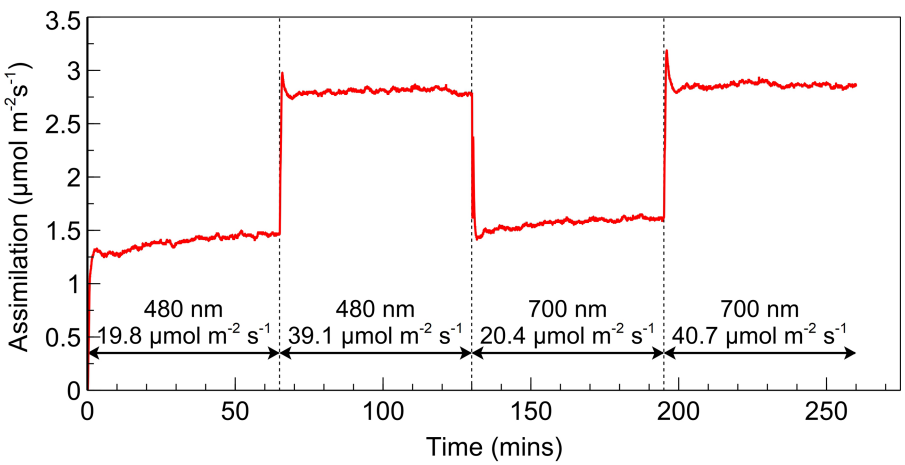

Figure 4. Response of assimilation to the doubling of intensity of PSI and PSII light.

Rate of assimilation for a SUN leaf initially exposed to PSII light at an absorbed irradiance of ~20 µmol m^{-2} s^{-1} followed by the subsequent doubling of intensity. PSII light was followed in the same manner by PSI light.

Biochemical Journal (2019) 476 3295–3312
https://doi.org/10.1042/BCJ20190576

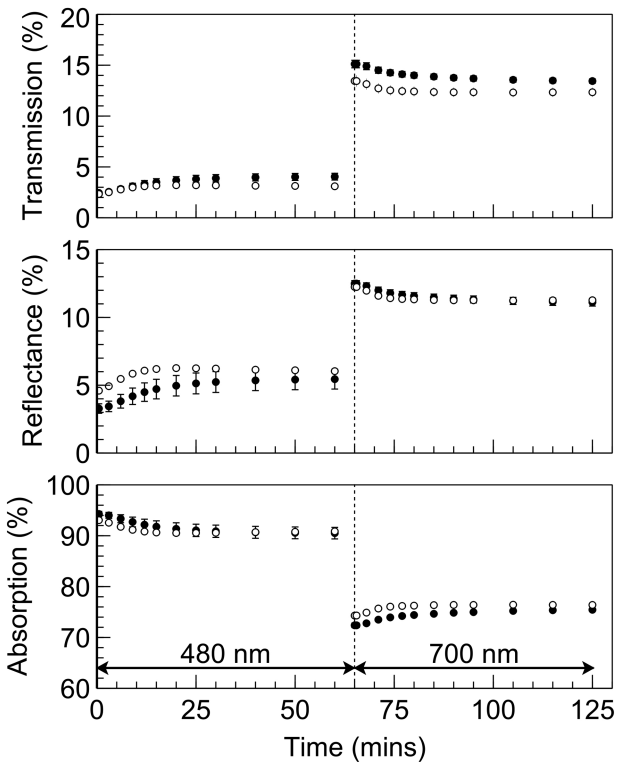

Figure 5. Leaf light transmission, reflectance and absorptance.
Leaf light transmission determined *in situ* on intact SUN (open circles) and SHADE (closed circles) leaves together with estimated reflection (based on transmission) and calculated absorption values. Error bars shown represent the SEM ($n = 3$).

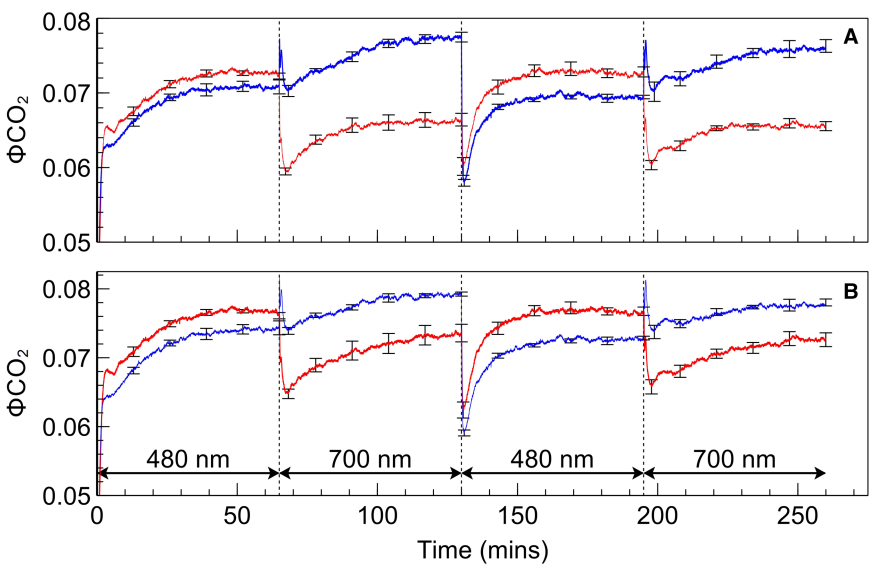

Figure 6. Φ_{CO2} traces during a PSII/PSI light regime.
Φ_{CO2} calculated for SUN (red) and SHADE (blue) leaves using (**A**) leaf absorption determined from leaf discs directly after gas exchange measurements or (**B**) calculated leaf absorption determined *in situ* on intact leaves during gas exchange measurements. Error bars shown represent the SEM ($n = 3$).

Biochemical Journal (2019) **476** 3295–3312
https://doi.org/10.1042/BCJ20190576

leaves are in state 1, creates a surge in fluorescence yield which is gradually quenched as the transition occurs to state 2. When switching from PSII light to PSI light, in contrast, fluorescence yield falls abruptly and subsequently increases during the transition to state 1. The responses of derived PSII parameters to PSII and PSI light are shown in Figures 8 (SUN leaves) and 9 (SHADE leaves), along with the response of Φ_{CO2} for the corresponding leaf type. Values for each fluorescence parameter (closed circles) are scaled and superimposed on the Φ_{CO2} traces to reveal the strong correlations between these data during exposure to either the PSII or PSI light.

Switching from PSII light to PSI light produced a prompt increase in Φ_{PSII} in SUN and SHADE leaves to just under 0.8; this increase was greater for the SHADE than for the SUN leaves due to the lower Φ_{PSII} in SHADE grown leaves under PSII light. Following the prompt change of Φ_{PSII} upon switching from PSII to PSI light there was only a slight subsequent slower increase in Φ_{PSII}. The changes in Φ_{PSII} produced upon changing from PSII to PSI light did not parallel the changes in Φ_{CO2}. The switch from PSI light to PSII light was accompanied by a prompt decrease in Φ_{PSII} to a global minimum in SUN (0.47) and SHADE (0.42) leaves followed by a slower increase to a stable value. The kinetics of the prompt decrease and subsequent slower recovery of Φ_{PSII} paralleled closely the changes in Φ_{CO2} produced by the irradiance changes, implying a close coupling between Φ_{CO2} and Φ_{PSII}. The extent of the prompt decrease in Φ_{PSII} was greater for the SHADE grown leaves (46% compared with 38% for SUN leaves) and the subsequent stable value of Φ_{PSII} reached after the slow increase was greater for the SUN grown leaves (~0.65 compared with ~0.6 for SHADE leaves).

Φ_{PSII} is the product of F′v/F′m, the quantum efficiency for electron transport by PSII when all reaction centres are open (strictly it is a relative quantum efficiency), and the photochemical efficiency factor, q_P [35], which is the factor by which PSII efficiency is decreased as a result of some Q_A being reduced and therefore traps being closed. Trap closure increases the trapping time and so increases the probability that the migrating excited state of chlorophyll *a* will be dissipated via a non-photochemical route, such as fluorescence or a non-photochemical quenching mechanism [36]. The changes of q_P and F′v/F′m after switching from PSII light to PSI light and back again are therefore relevant to understanding the changes in Φ_{PSII}. Qualitatively, the changes in q_P are similar to the changes in Φ_{PSII}; following a change from PSII light to PSI light q_P rises to a value close to one in both SUN and SHADE grown leaves and thereafter remains stable and does not track the changes in $\Phi_{CO2,}$ while after the change from PSI light to PSII light q_P decreases promptly and then increases slowly in parallel with Φ_{CO2}. F′v/F′m in SUN and SHADE grown leaves increases slightly (by ~0.02) upon changing from PSII light to PSI light, and decreases slightly (by ~0.02) upon transferring from PSI light to PSII light. In both SUN and SHADE grown leaves after a PSII light to PSI light change the increase in F′v/F′m tracks the increase in Φ_{CO2}. Upon switching from PSI light to PSII light F′v/F′m decreases while Φ_{CO2} increases; in SUN grown leaves these corresponding changes are weakly correlated whereas in SHADE grown leaves no correlation exists. The ratio of light-adapted maximum fluorescence to dark-adapted maximum

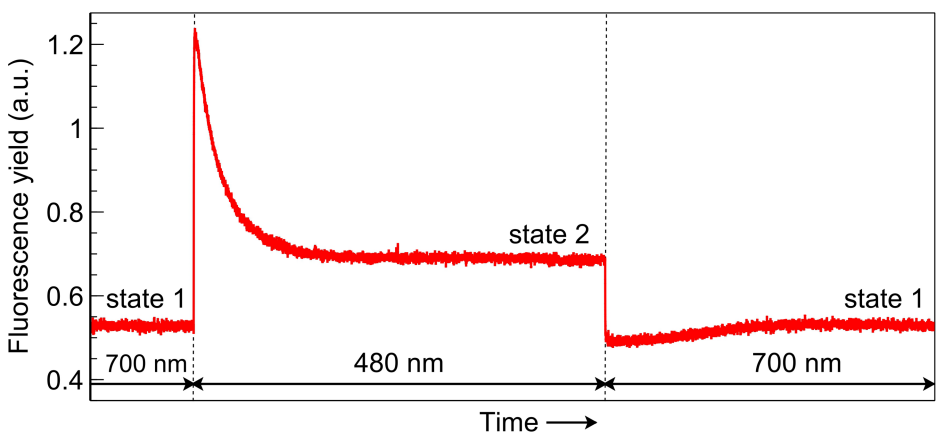

Figure 7. Fluorescence yield associated with transitions between state 1 and state 2.

Segment of fluorescence yield trace obtained with a SUN leaf and bearing classical hallmarks of a state transition. Fluorescence yield changes abruptly upon light switching and subsequent increases or decreases to a new steady state as a state transition proceeds.

Biochemical Journal (2019) 476 3295–3312
https://doi.org/10.1042/BCJ20190576

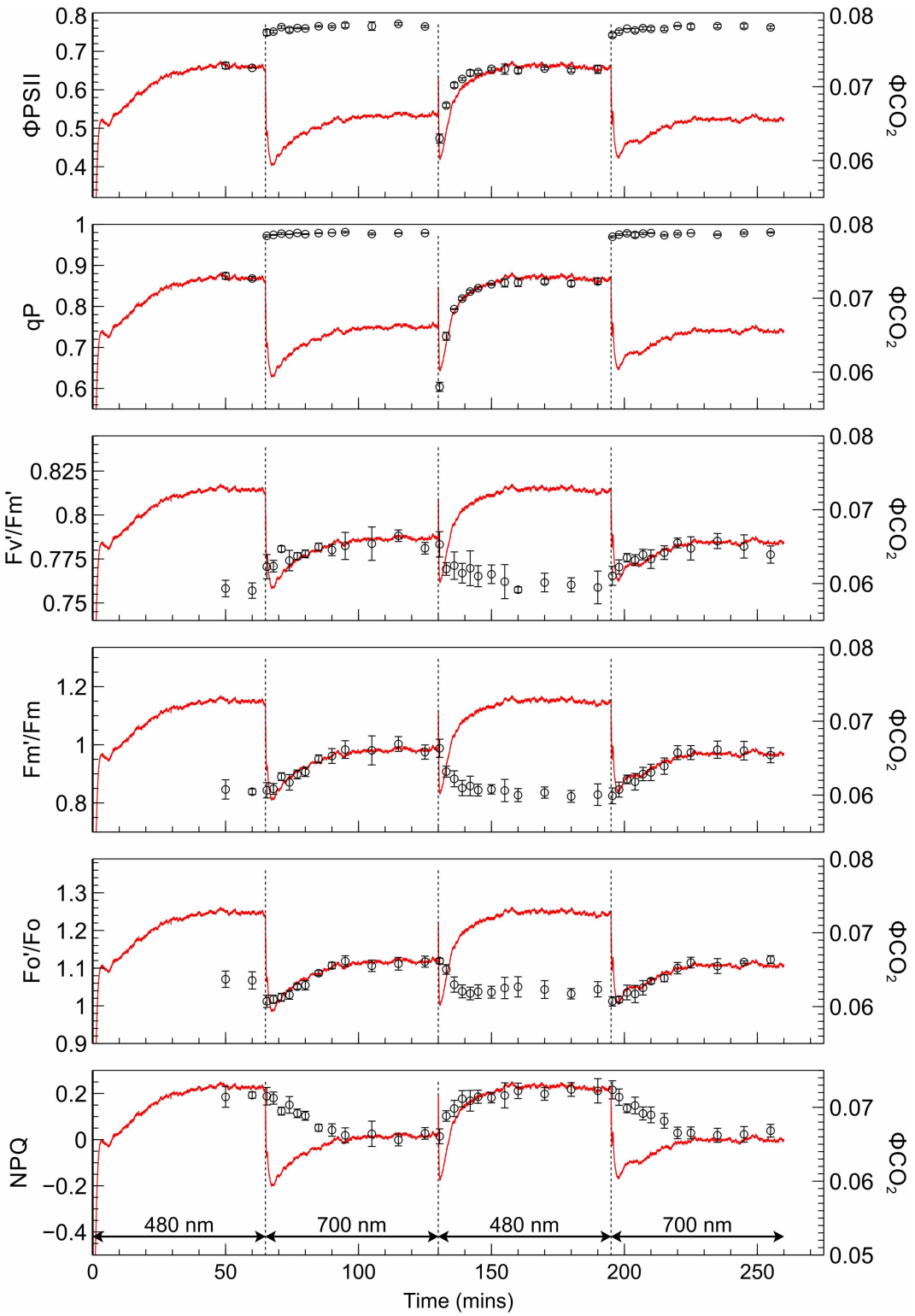

Figure 8. Responses of selected fluorescence parameters to a PSII/PSI light regime in SUN leaves, superimposed over corresponding scaled Φ_{CO2} responses.

Measurements of ΦPSII, q_P, F′m/Fm, F′o/Fo, F′v/F′m, and NPQ (open circles) for SUN leaves, superimposed on light-limited Φ_{CO2} traces for SUN leaves. Error bars shown represent the SEM ($n = 3$).

Biochemical Journal (2019) **476** 3295–3312
https://doi.org/10.1042/BCJ20190576

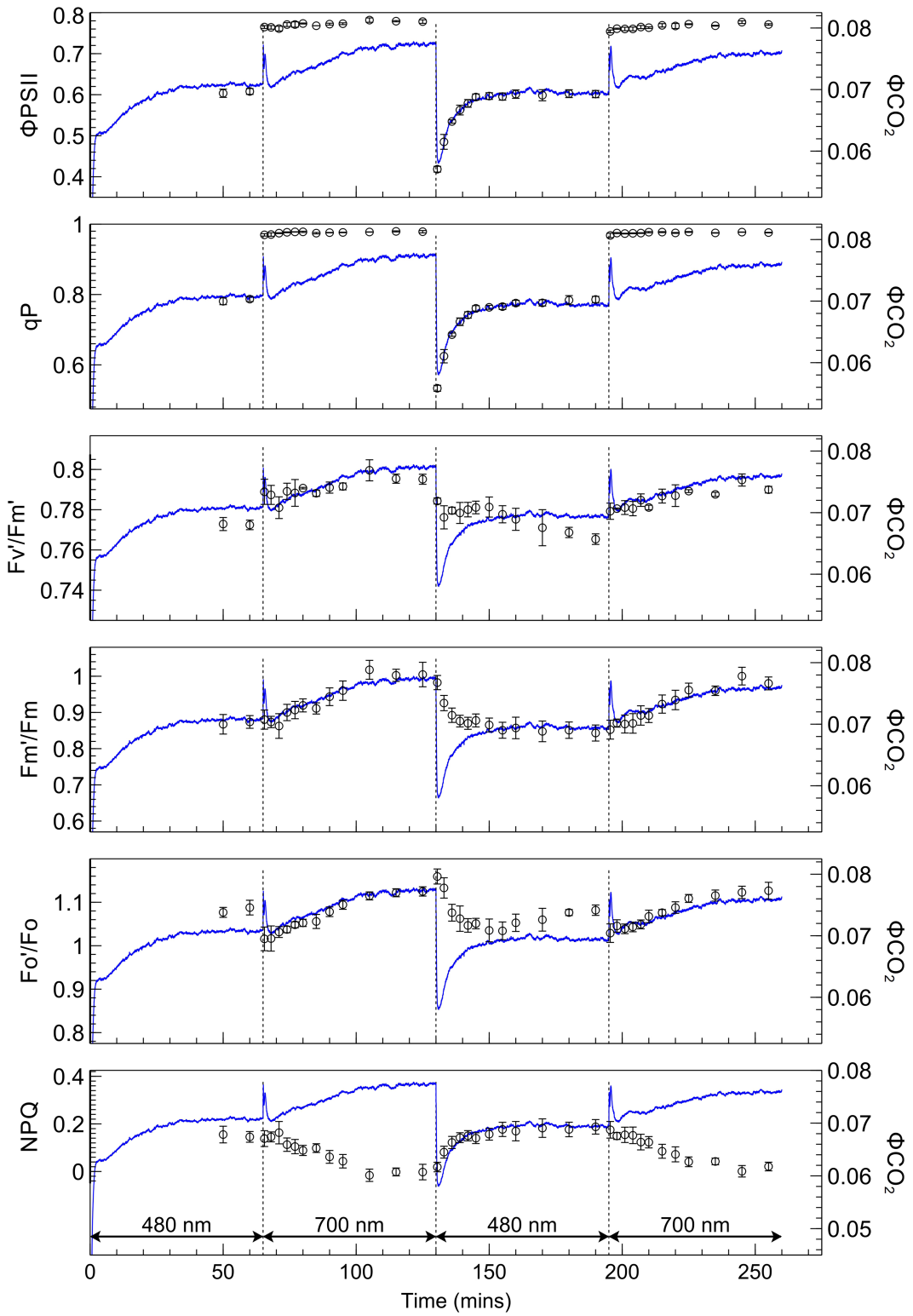

Figure 9. Responses of selected fluorescence parameters to a PSII/PSI light regime in SHADE leaves, superimposed over corresponding scaled Φ_{CO2} responses.

Measurements of ΦPSII, q_P, F′m/Fm, F′o/Fo, F′v/F′m, and NPQ (open circles) for SHADE leaves, superimposed on light-limited Φ_{CO2} traces for SUN leaves. Error bars shown represent the SEM ($n = 3$).

Biochemical Journal (2019) **476** 3295–3312
https://doi.org/10.1042/BCJ20190576

fluorescence (F′m/Fm) increases after a PSII light to PSI light transition by 16% in SUN leaves and 15% in SHADE leaves, indicating corresponding increases in PSII antennae size, and these increases track the increase in Φ_{CO2}. Corresponding increases in the minimum fluorescence equivalent (F′o/Fo) were 13% in SUN leaves and 10% in SHADE leaves. F′m/Fm and F′o/Fo decrease after a PSI to PSII light transition and are negatively

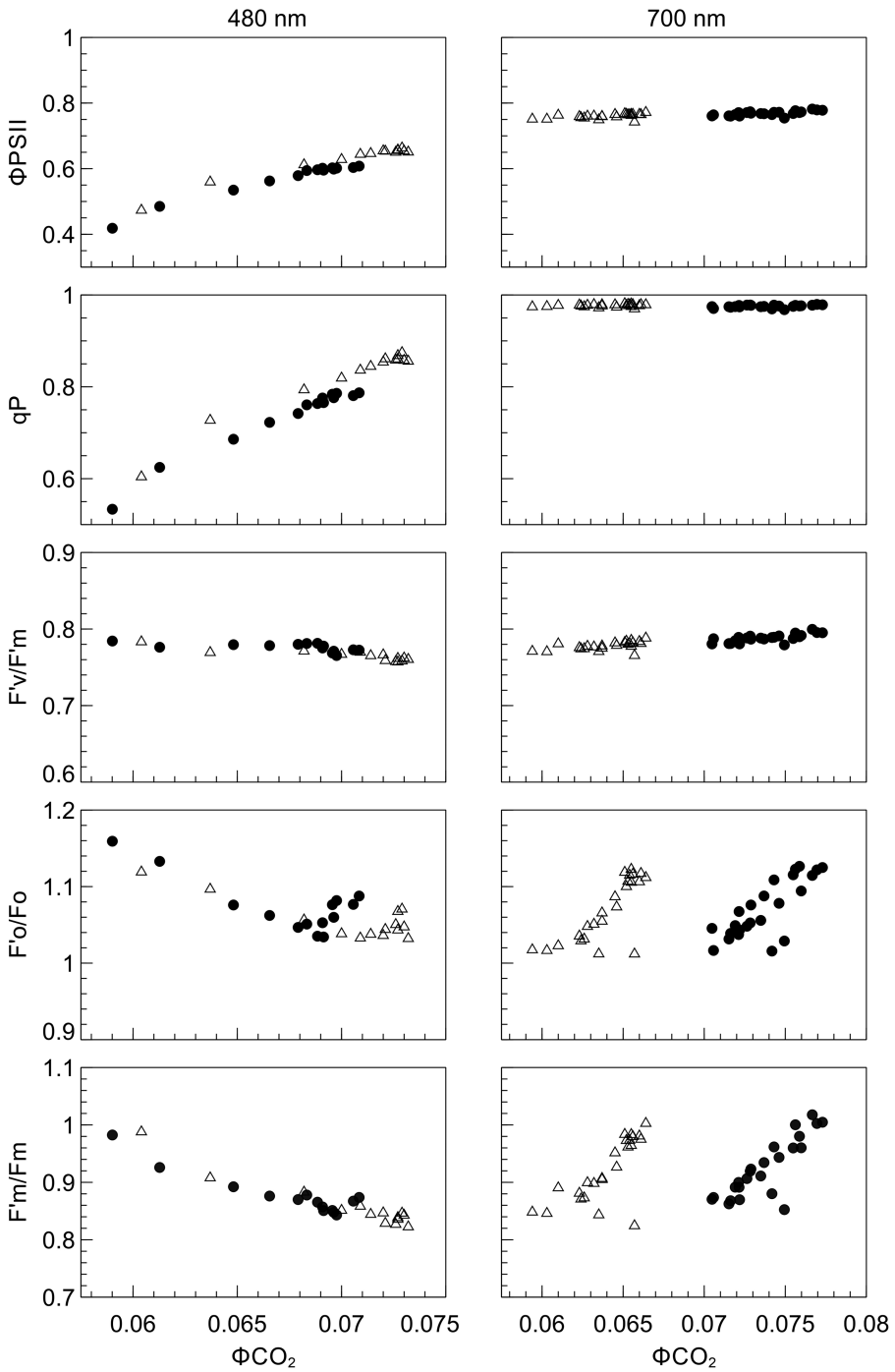

Figure 10. Relationship between selected fluorescence parameters and Φ_{CO2} during exposure of SUN and SHADE leaves to PSI (700 nm) or PSII (480 nm) light.

Relationship between Φ_{CO2} and ΦPSII, q_P, F′v/Fm, and F′o/Fo, F′m/Fm for SUN (open triangles) and SHADE leaves (closed circles) presented with 480 and 700 nm irradiance ($n = 3$).

Biochemical Journal (2019) 476 3295–3312
https://doi.org/10.1042/BCJ20190576

correlated with the subsequent increase in Φ_{CO2}. These decreases in F′m/Fm were 16% for SUN leaves and 14% for SHADE leaves while corresponding decreases in F′o/Fo were 7% for SUN and SHADE leaves. NPQ (Fm/F′m − 1) increases after a PSI to PSII light transition, tracking the increase in Φ_{CO2}, and is negatively correlated with increases in Φ_{CO2} following a PSII light to PSI light transition.

The relationship between fluorescence parameters and Φ_{CO2} were examined in further detail by plotting each fluorescence-derived parameter against Φ_{CO2} (Figure 10). In SUN and SHADE leaves subjected to PSI light, the increase in Φ_{CO2} as the transition from state 1 to state 2 proceeded was not accompanied by changes in Φ_{PSII} or q_P. When these leaf types were exposed to PSII light, however, increases in Φ_{CO2} were accompanied by corresponding increases in Φ_{PSII} and q_P. In SHADE leaves the PSI-light data points are right-shifted and the PSII light data points are left-shifted compared with SUN leaves. No significant changes in F′v/F′m occurred during either a state 1 to state 2 transition or a state 2 to state 1 transition. Parameters F′o/Fo and F′m/Fm were positively related to Φ_{CO2} under PSII light but negatively related to Φ_{CO2} under PSI light, implying an effect of PSII cross-sectional area on Φ_{CO2}.

Discussion

We present compelling evidence for the first time of a relationship between state transitions and photosynthetic efficiency in a higher plant. State transitions are known to occur in algae, cynaobacteria, and higher plants but until now an accompanying increase in photosynthetic efficiency during a state transition had been observed only in algae and cyanobacteria [13–15,19]. A relationship between state transitions and photosynthetic efficiency is predicted if the widely held view of state transitions as a short-term energy redistribution mechanism is to be accepted. The absence of such a relationship in higher plants has created difficulty in understanding the functional significance of state transitions in leaves. In the present study, SUN and SHADE leaves were subjected to a sequence of PSI and PSII light known to result in closely matched rates of assimilation at a steady state. Switching between each light type was followed by a drop in assimilation rate and a subsequent increase to a steady state occurring over ∼30 min.

Changes in F′m/Fm and F′o/Fo, which correspond to changes in PSII antennae size expected to occur during a state transition, closely tracked changes in Φ_{CO2} in SUN and SHADE leaves; Φ_{CO2} is a measure of the integrated light-use efficiency of photosynthesis, including PSII and PSI. If F′m/Fm is considered as directly proportional to PSII cross-sectional area [20] then the latter decreased by 16% in SUN leaves and 14% in SHADE leaves during the transition from state 1 to state 2 under PSII light. These figures lie between a reported 11% decrease in PSII antennae size for Arabidopsis [21] and a ∼20% decrease in spinach [22], and the mobile LHC pool size determined in the present study is thus also less than a figure of 20% reported for maize [37]. These decreases in PSII antennae size which we observed (and subsequent increases) represent fully reversible binary states, consistent with the reversible nature of state transitions. Since Φ_{CO2} increases after a switch to PSII light, while PSII antennae size decreases, this raises the question about the docking location of mobile LHCII which detaches from PSII. While this study has not directly resolved this question, it has established that the reorganisation at the molecular level following a switch from PSI to PSII light (state 1 to state 2) partially alleviates a limitation that affects Φ_{CO2} and thus produces an increase in photosynthetic light-use efficiency. Andrews et al. [15] observed small increases in Φ_{PSI} following a switch from PSII to PSI light, implying that the rate of electron turnover through PSI is the limitation. The findings by those authors fits well with the view that PSI is the docking location of mobile LHCII in state 2 [25,26] but conflicting findings exist in the literature (e.g. [24]). In the present study, the increase in Φ_{CO2} with a decrease in PSII antenna size (e.g. a decrease in F′m/Fm) would be consistent with a detachment of LHCII from PSII and its attachment to PSI, resulting in an increase in the combined light-use efficiency for linear electron transport.

State transitions were accompanied by small changes in F′v/F′m which indicate that changes in the efficiency with which an electron was transferred to PSII occurred during state transitions. F′v/F′m increased upon exposure to PSI light when a state 2 to state 1 transition occurred and it decreased (abruptly) under PSII light when a state 1 to state 2 transition occurred. The same pattern was observed in wheat leaves exposed to a similar PSI/PSII light regime [15]. Those authors suggested that changes in non-photochemical quenching, possibly through modification of PSII antennae, as a possible cause for the observed changes in F′v/F′m. Indeed, in the present study, steady state NPQ decreased from ∼0.2 in leaves exposed to PSII light to zero in leaves exposed to PSI light, but such a change would be expected as the result of a decrease in the PSII antenna size occurring as a result of LHCII movement. A possible explanation for the decrease in F′v/F′m following exposure to PSII light is that any attachment of LHCII to PSI would increase the amount of PSI fluorescence. PSI fluorescence

Biochemical Journal (2019) 476 3295–3312
https://doi.org/10.1042/BCJ20190576

contributes to both the Fo or F′o (e.g. [2]) and the Fm or F′m fluorescence yields, but the relative contribution to the Fo and F′o signals is greater (e.g. [38]) so any increase in PSI fluorescence would be expected to decrease F′v/F′m so this change is consistent with a state transition detaching LHCII from PSII followed by its attachment to PSI.

Following exposure to PSII light Φ_{CO2} increases in parallel with Φ_{PSII} and these changes in Φ_{PSII} are largely due to q_P as the changes in F′v/F′m were small. The changes in q_P are due to the decrease in PSII antenna size (F′m/Fm decreases) and probably the increase in PSI antenna size. Correlation of the flux of electrons through PSII with that of the demand of reductant for CO_2 fixation can often be done with reference to Φ_{PSII} alone (e.g. [35,39]). In this case, however, the changing antenna size of PSII during exposure to PSII light means that PSII electron transport is not governed by changes only in Φ_{PSII} as this measure includes no direct involvement of antenna size.

We used SUN and SHADE leaves to explore the potential impact of considerably different growth spectra on state transitions. Whereas the SUN leaves were produced under a spectrum which preferentially excites PSII (PSII light), SHADE leaves were produced under a spectrum which preferentially excites PSI (PSI light). The different leaf types displayed the 'memory' of growth spectra with respect to growth irradiance; SHADE leaves utilised the PSI light more efficiently (∼16%) than SUN leaves whereas SUN leaves utilised PSII light only slightly more efficiently (∼3%) than SHADE leaves. The higher chlorophyll *a*/*b* ratio of SUN leaves compared with that of SHADE leaves is indicative of a higher PSI/PSII ratio in SUN leaves (and lower PSI/PSII ratio in SHADE leaves) [7,40] which is consistent with the differences in light-use efficiency with respect to light type observed in the present study. The difference between leaf types in terms of the efficiency of PSI and PSII light utilisation is further illustrated by plotting Φ_{CO2} (*x*-axis) against Φ_{PSII} (*y*-axis); data points for SUN leaves corresponding with PSII light are right-shifted compared with that for SHADE leaves and the opposite is true for the PSI light points. The same 'memory' of growth spectrum has been found to occur in leaves as a result of long-term acclimatory processes that tune photosystem stoichiometry to growth spectrum [6,7]. Clearly, state transitions are capable of mitigating, but not eliminating, losses in Φ_{CO2} arising from imbalanced photosystem excitation; as in cucumber leaves produced under the same artificial sun and shade growth spectra the PSII acceptor side remains strongly reduced in state 2 [7]. This is consistent with the view of state transitions as a 'fine-tuning' energy redistribution mechanism [41]. In terms of the extent of state transition and $\Delta\Phi_{CO2}$ in the two leaf types, $\Delta\Phi_{CO2}$ during the transition from state 2 to state 1 was ∼10% and ∼13% during a transition from state 1 to state 2 in both leaf types. The similar changes in $\Delta\Phi_{CO2}$ are proportional to corresponding changes in antennae size of PSII and suggest that growth history does not affect the size of the mobile LHCII pool or its effect on $\Delta\Phi_{CO2}$.

The reasons why we observed a recovery in overall photosynthetic light-use efficiency (i.e. Φ_{CO2}) upon light switching while Andrews et al. [15] did not cannot be resolved in the present study. However, our fluorescence results bear striking resemblance to those presented in their study in terms of characteristics and extent upon light switching. On the other hand, our results are in agreement with Bonaventura and Myers [13] who observed a recovery in the rate of oxygen evolution which they note had similar kinetics to that of fluorescence yield. In *Chlamydomonas*, a greater proportion of LHCII is mobile than in higher plants, possibly as a result of the lower amount of thylakoid stacking in *Chlamydomonas* compared with higher plants which makes LHCII more accessible for phosphorylation kinases [42]. At least in tomato, we show that changes in assimilation track changes in the fluorescence-derived parameters characteristic of state transitions, which implies that assimilation measurements could be used to measure state transitions in leaves.

Detailed analysis of the spikes in assimilation which occurred upon switching from PSII to PSI light revealed more intricate bimodal assimilation kinetics. To exclude a spike in actinic light intensity or any other spurious in light intensity upon light switching as the cause of these kinetics, a high-speed photodiode light monitoring circuit connected to an oscilloscope was used to probe light intensity upon light switching. It was found that light intensity ramped up (and down) to the desired intensity for PSI and PSII light within a matter of microseconds and no overshoot occurred. The observed kinetics in assimilation are therefore physiological in nature. When switching from PSII light to PSI light the PQ pool is rapidly oxidised and during this very brief period, a greater flux of electrons flows through PSI. This creates a temporarily better balanced flux of electrons through the photosystems which results in a brief spike in assimilation rate. The principle of this mechanism is therefore related to the Emerson enhancement effect [43,44]. The 'residual enhancement effect' which we observed in the present study shows that, under unique conditions, enhancement can be a brief artefact of previous irradiance conditions due to the capacitive nature of the PQH_2 pool.

The ability to observe state transitions by relatively straightforward gas exchange and fluorescence methods creates a new avenue to explore the link between photosystem organisation and CO_2 assimilation. Whether this relationship is preserved in a natural, ecophysiological context, remains to be elucidated.

Abbreviations

ATP, adenosine triphosphate; Fd, ferredoxin; Fm, dark-adapted maximum fluorescence; F′m, light-adapted maximum fluorescence; Fo, dark-adapted minimum fluorescence; F′o, light-adapted minimum fluorescence; F′v/F′m, maximum light-adapted efficiency of PSII; LHCII, light-harvesting complex II; NADPH, nicotinamide adenine dinucleotide phosphate; P700, photosystem I primary donor; PCB, printed circuit board; PQ, plastoquinone; PSI, photosystem I; PSII, photosystem II; Q_A, primary quinone acceptor of PSII; SEM, standard error of the mean; Φ_{CO2}, light-limited quantum yield of CO_2 fixation; Φ_{PSII}, quantum yield of PSII electron transport.

Author contributions

C.R.T., W.v.I and J.H. designed the research. C.R.T. performed research and analysed data. C.R.T. and J.H. wrote the article.

Funding

This work was funded by the Biosolar consortium.

Acknowledgements

The authors wish to extend their gratitude to Emilie Wientjes for providing chlorophyll *a/b* data, Maarten Wassenaar for his technical assistance, and Marcel Krijn and Eugen Onac from Philips Electronics B.V. for providing optical equipment for calibration of the laboratory-built light sensor. With additional support from Philips Electronics B.V. and Plant Dynamics B.V.

Competing Interests

The Authors declare that there are no competing interests associated with the manuscript.

References

1 Foyer, C.H., Neukermans, J., Queval, G., Noctor, G. and Harbinson, J. (2012) Photosynthetic control of electron transport and the regulation of gene expression. *J. Exp. Bot.* **63**, 1637–1661 https://doi.org/10.1093/jxb/ers013
2 Pfündel, E. (1998) Estimating the contribution of photosystem I to total leaf chlorophyll fluorescence. *Photosynth. Res.* **56**, 185–195 https://doi.org/10.1023/A:1006032804606
3 Laisk, A., Vello, O., Eichelmann, H. and Dall'Osto, L. (2014) Action spectra of photosystems II and I and quantum yield of photosynthesis in leaves in State 1. *Biochim. Biophys. Acta* **1837**, 315–325 https://doi.org/10.1016/j.bbabio.2013.12.001
4 Croce, R., Müller, M.G., Bassi, R. and Holzwarth, A.R. (2001) Carotenoid-to-chlorophyll energy transfer in recombinant major light-harvesting complex (LHCII) of higher plants. I. Femtosecond transient absorption measurements. *Biophys. J.* **80**, 901–915 https://doi.org/10.1016/S0006-3495(01)76069-9
5 Holmes, M.G. and Smith, H. (1977) The function of phytochrome in the natural environment—I. Characterization of daylight for studies in photomorphogenesis and photoperiodism. *Photochem. Photobiol.* **25**, 533–538 https://doi.org/10.1111/j.1751-1097.1977.tb09124.x
6 Chow, W.S., Melis, A. and Anderson, J.M. (1990) Adjustments of photosystem stoichiometry in chloroplasts improve the quantum efficiency of photosynthesis. *Proc. Natl Acad. Sci. U.S.A.* **87**, 7502–7506 https://doi.org/10.1073/pnas.87.19.7502
7 Hogewoning, S.W., Wientjes, E., Douwstra, P., Trouwborst, G., van Ieperen, W., Croce, R. et al. (2012) Photosynthetic quantum yield dynamics: from photosystems to leaves. *Plant Cell* **24**, 1921–1935 https://doi.org/10.1105/tpc.112.097972
8 Myers, J. (1971) Enhancement studies in photosynthesis. *Annu. Rev. Plant Biol.* **22**, 289–312 https://doi.org/10.1146/annurev.pp.22.060171.001445
9 Allen, J.F., Bennett, J., Steinback, K.E. and Arntzen, C.J. (1981) Chloroplast protein phosphorylation couples plastoquinone redox state to distribution of excitation energy between photosystems. *Nature* **291**, 25–29 https://doi.org/10.1038/291025a0
10 Bellafiore, S., Barneche, F., Peltier, G. and Rochaix, J. (2005) State transitions and light adaptation require chloroplast thylakoid protein kinase STN7. *Nature* **433**, 892–895 https://doi.org/10.1038/nature03286
11 Pribil, M., Pesaresi, P., Hertle, A., Barbato, R. and Leister, D. (2010) Role of plastid phosphatase TAP38 in LHCII dephosphorylation and thylakoid electron flow. *PLOS Biol.* **8**, e1000288 https://doi.org/10.1371/journal.pbio.1000288
12 Shapiguzov, A., Ingelsson, B., Samol, I., Andres, C., Kessler, F., Rochaix, J.-D. et al. (2010) The PPH1 phosphatase is specifically involved in LHCII dephosphorylation and state transitions in Arabidopsis. *Proc. Natl Acad. Sci. U.S.A.* **107**, 4782–4787 https://doi.org/10.1073/pnas.0913810107
13 Bonaventura, C. and Myers, J. (1969) Fluorescence and oxygen evolution from *Chlorella pyrenoidosa*. *Biochim. Biophys. Acta* **189**, 366–383 https://doi.org/10.1016/0005-2728(69)90168-6
14 Murata, N. (1969) Control of excitation transfer in photosynthesis. 1. Light-induced change of chlorophyll *a* fluorescence in *Porphyridium cruentum*. *Biochim. Biophys. Acta* **172**, 242–251 https://doi.org/10.1016/0005-2728(69)90067-X
15 Andrews, J.R., Bredenkamp, G.J. and Baker, N.R. (1993) Evaluation of the role of State transitions in determining the efficiency of light utilisation for CO_2 assimilation in leaves. *Photosynth. Res.* **38**, 15–26 https://doi.org/10.1007/BF00015057

Biochemical Journal (2019) **476** 3295–3312
https://doi.org/10.1042/BCJ20190576

16 Delosme, R., Olive, J. and Wollman, F.-A. (1996) Changes in light energy distribution upon state transitions: an in vivo photoacoustic study of the wild type and photosynthesis mutants from *Chlamydomonas reinhardtii*. *Biochim. Biophys. Acta* **1273**, 150–158 https://doi.org/10.1016/0005-2728(95)00143-3
17 Canaani, S. and Malkin, S. (1984) Distribution of light excitation in an intact leaf between the two photosystems of photosynthesis. Changes in absorption cross-sections following state 1-state 2 transitions. *Biochim. Biophys. Acta* **766**, 513–524 https://doi.org/10.1016/0005-2728(84)90109-9
18 Veeranjaneyulu, K. and Leblanc, R.M. (1994) Action spectra of photosystems I and II in state 1 and state 2 in intact sugar maple leaves. *Plant Physiol.* **104**, 1209–1214 https://doi.org/10.1104/pp.104.4.1209
19 Canaani, O. (1986) Photoacoustic detection of oxygen evolution and State 1–State 2 transitions in cyanobacteria. *Biochim. Biophys. Acta* **852**, 74–80 https://doi.org/10.1016/0005-2728(86)90058-7
20 Allen, J.F. (1992) Protein phosphorylation in regulation of photosynthesis. *Biochim. Biophys. Acta* **1098**, 275–335 https://doi.org/10.1016/S0005-2728(09)91014-3
21 Kim, E., Ahn, T.K. and Kumazaki, S. (2015) Changes in antenna sizes of photosystems during state transitions in granal and stroma-exposed thylakoid membrane of intact chloroplasts in Arabidopsis mesophyll protoplasts. *Plant Cell Physiol.* **56**, 759–768 https://doi.org/10.1093/pcp/pcv004
22 Forti, G. and Fusi, P. (1990) Influence of thylakoid protein phosphorylation on Emerson enhancement and the quantum requirement of Photosystem I. *Biochim. Biophys. Acta* **1020**, 247–252 https://doi.org/10.1016/0005-2728(90)90154-V
23 Telfer, A., Whitelegge, J.P., Bottin, H. and Barber, J. (1986) Changes in the efficiency of P700 photo-oxidation in response to protein phosphorylation detected by flash absorption spectroscopy. *J. Chem. Soc. Faraday Trans.* **82**, 2207–2215 https://doi.org/10.1039/f29868202207
24 Haworth, P. and Melis, A. (1983) Phosphorylation of chloroplast thylakoid membrane proteins does not increase the absorption cross-section of photosystem 1. *FEBS Lett.* **160**, 277–280 https://doi.org/10.1016/0014-5793(83)80982-X
25 Ünlü, C., Drop, B., Croce, R. and van Amerongen, H. (2014) State transitions in *Chlamydomonas reinhardtii* strongly modulate the functional size of photosystem II but not of photosystem I. *Proc. Natl Acad. Sci. U.S.A.* **111**, 3460–3465 https://doi.org/10.1073/pnas.1319164111
26 Galka, P., Santabarbara, S., Khuong, T.T.H., Degand, H., Morsomme, P., Jennings, R.C. et al. (2012) Functional analyses of the plant photosystem I–light-harvesting complex II supercomplex reveal that light-harvesting complex II loosely bound to photosystem II is a very efficient antenna for photosystem I in State II. *Plant Cell* **24**, 2963–2978 https://doi.org/10.1105/tpc.112.100339
27 Wientjes, E., van Amerongen, H. and Croce, R. (2013) LHCII is an antenna of both photosystems after long-term acclimation. *Biochim. Biophys. Acta* **1827**, 420–426 https://doi.org/10.1016/j.bbabio.2012.12.009
28 Wagner, R., Dietzel, L., Bräutigam, K., Fischer, W. and Pfannschmidt, T. (2008) The long-term response to fluctuating light quality is an important and distinct light acclimation mechanism that supports survival of *Arabidopsis thaliana* under low light conditions. *Planta* **228**, 573–587 https://doi.org/10.1007/s00425-008-0760-y
29 Frenkel, M., Bellafiore, S., Rochaix, J.-D. and Jansson, S. (2007) Hierarchy amongst photosynthetic acclimation responses for plant fitness. *Physiol. Plant.* **129**, 455–459 https://doi.org/10.1111/j.1399-3054.2006.00831.x
30 Dietzel, L., Bräutigam, K. and Pfannschmidt, T. (2008) Photosynthetic acclimation: state transitions and adjustment of photosystem stoichiometry – functional relationships between short-term and long-term light quality acclimation in plants. *FEBS J.* **275**, 1080–1088 https://doi.org/10.1111/j.1742-4658.2008.06264.x
31 Hogewoning, S.W., Trouwborst, G., Harbinson, J. and Van Ieperen, W. (2010) Light distribution in leaf chambers and its consequences for photosynthesis measurements. *Photosynthetica* **48**, 219–226 https://doi.org/10.1007/s11099-010-0027-2
32 Maxwell, K. and Johnson, G.N. (2000) Chlorophyll fluorescence — a practical guide. *J. Exp. Bot.* **51**, 659–668 https://doi.org/10.1093/jexbot/51.345.659
33 Kok, B. (1948) A critical consideration of the quantum yield of Chlorella photosynthesis. *Enzymologia* **13**, 1–56
34 Croce, R., Canino, G., Ros, F. and Bassi, R. (2002) Chromophore organization in the higher-plant photosystem II antenna protein CP26. *Biochemistry* **41**, 7334–7343 https://doi.org/10.1021/bi0257437
35 Genty, B., Briantais, J.-M. and Baker, N.R. (1989) The relationship between the quantum yield of photosynthetic electron transport and quenching of chlorophyll fluorescence. *Biochim. Biophys. Acta* **990**, 87–92 https://doi.org/10.1016/S0304-4165(89)80016-9
36 Hendrickson, L., Furbank, R.T. and Chow, W.S. (2004) A simple alternative approach to assessing the fate of absorbed light energy using chlorophyll fluorescence. *Photosynth. Res.* **82**, 73–81 https://doi.org/10.1023/B:PRES.0000040446.87305.f4
37 Bassi, R., Rigoni, F., Barbato, R. and Giacometti, G.M. (1988) Light-harvesting chlorophyll a/b proteins (LHCII) populations in phosphorylated membranes. *Biochim. Biophys. Acta* **936**, 29–38 https://doi.org/10.1016/0005-2728(88)90248-4
38 Harbinson, J. (2018). Chlorophyll fluorescence as a tool for describing the operation and regulation of photosynthesis in vivo. In *Light Harvesting in Photosynthesis* (Croce, R., Grondelle, R.V., Amerongen, H.V. and Stokkum, I.V., eds), CRC Press, Boca Raton
39 Genty, B. and Harbinson, J. (1996). Regulation of light utilization for photosynthetic electron transport. In *Photosynthesis and the Environment* (Baker, N. R., ed), pp. 67–99, Kluwer Academic Publishers, Dordrecht, The Netherlands
40 Melis, A. and Harvey, G.W. (1981) Regulation of photosystem stoichiometry, chlorophyll a and chlorophyll b content and relation to chloroplast ultrastructure. *Biochim. Biophys. Acta* **637**, 138–145 https://doi.org/10.1016/0005-2728(81)90219-X
41 Anderson, J., Chow, W.H. and Park, Y.I. (1995) The grand design of photosynthesis: acclimation of the photosynthetic apparatus to environmental cues. *Photosynth. Res.* **46**, 129–139 https://doi.org/10.1007/BF00020423
42 Dekker, J.P. and Boekema, E.J. (2005) Supramolecular organization of thylakoid membrane proteins in green plants. *Biochim. Biophys. Acta* **1706**, 12–39 https://doi.org/10.1016/j.bbabio.2004.09.009
43 Emerson, R. (1957) Dependence of yield of photosynthesis in long wave red on wavelength and intensity of supplementary light. *Science* **125**, 746–752 https://doi.org/10.1126/science.125.3251.746
44 Emerson, R. (1958) Yield of photosynthesis from simultaneous illumination with pairs of wavelengths. *Science* **127**, 1059–1060